Resolving the Types and Origin of Active Oxygen Species Present in Supported Mn-Na_2WO_4/SiO_2 Catalysts for Oxidative Coupling of Methane

Sagar Sourav[1, 2], Yixiao Wang[1,*], Daniyal Kiani[2], Jonas Baltrusaitis[2,*], Rebecca R. Fushimi[1,*] and Israel E. Wachs[2,*]

[1]Biological and Chemical Science and Engineering, Energy Environment Science & Technology, Idaho National Laboratory, Idaho Falls, ID, 83415 USA

[2]Department of Chemical and Biomolecular Engineering, Lehigh University, Bethlehem, PA, 18015 USA

*Corresponding Authors: yixiao.wang@inl.gov, job314@lehigh.edu, rebecca.fushimi@inl.gov, iew0@lehigh.edu

1. Experimental

a. Catalyst Synthesis

The SiO_2 support (Cabot CAB-O-SIL® EH5, SA ~332 m^2/g) was hydrolyzed by adding excess water, which was then allowed to dry overnight at room temperature before final calcination at 500 °C for 4 hours under constant air flow. The flakes of SiO_2 thus obtained were then crushed and sieved to form fine powder like particles of size 100-150 μm.

The catalysts were synthesized by incipient wetness impregnation method. For this purpose, the pore volume of the SiO_2 support was calculated to be ~ 0.8 mL/g of SiO_2. The following metal oxide precursors were used for the catalyst synthesis: $Na_2WO_4{\cdot}2H_2O$, Sigma Aldrich, 99%; $Mn(NO_3)_2{\cdot}6H_2O$, Alfa Aesar, 99.98%; NaOH, Fisher Scientific, 97.8%; ammonium metatungstate, Pfaltz & Bauer, 99.5%. For the preparation of $5Na_2WO_4/SiO_2$ catalyst, desired amount of aqueous solution of $Na_2WO_4{\cdot}2H_2O$ was dropwise added to the SiO_2 support. For the preparation of $1.2Mn/SiO_2$ catalyst, aqueous solution of $Mn(NO_3)_2{\cdot}6H_2O$ was utilized. For the preparation of $0.5Na\text{-}5WO_x/SiO_2$ catalyst, NaOH and ammonium metatungstate were chosen as the source precursors of Na and W-oxides, respectively. In this case, the aqueous solution of desired amount of these oxide precursors was dropwise added to the SiO_2 support. In all cases, the catalyst samples were dried over night at room temperature after the impregnation. In the case of $1.2Mn\text{-}5Na_2WO_4/SiO_2$ catalyst, a two-step impregnation was followed. First, the desired amount of aqueous solution of $Na_2WO_4{\cdot}2H_2O$ was added to the SiO_2 support. Then the sample was dried overnight at room temperature. Following the drying process, aqueous solution of $Mn(NO_3)_2{\cdot}6H_2O$ was added to the above sample and was dried again over night at room temperature. Finally, all the samples were dried further at 120 °C for 2 hours and then calcined at 800 °C for 8 hours under continuous air flow. The weight loading of the active metal components in the catalyst can be inferred from its nomenclature. For example, $1.2Mn\text{-}5Na_2WO_4/SiO_2$ catalyst contains 1.2 wt.% of Mn and 5 wt.% of Na_2WO_4 active phases.

To study the effect of cristobalite support, $0.8Na/SiO_2$ (0.8 wt.% Na is the equivalent to the amount of Na present in $5Na_2WO_4/SiO_2$ and $1.2Mn\text{-}5Na_2WO_4/SiO_2$ catalysts) sample was also synthesized to transform

the amorphous SiO_2 phase to the crystalline cristobalite phase. In this case, the desired amount of Na was impregnated into the SiO_2 support by the aqueous solution of NaOH. The drying and calcination of this sample was carried out as described above, except the calcination was carried out at a higher temperature, 900 °C. To study the effect of "amorphous bare SiO_2 Support" the water-treated (treatment procedure is described above) SiO_2 was used.

For Raman spectroscopy structural analysis, the final calcined powder catalysts were used. For temporal analysis of products (TAP) experiments, the catalyst powder samples were pressed and then crushed and sieved to form particles of size 250-300 μm.

b. *In-situ* Raman Spectroscopy

The *in-situ* Raman spectra of the catalysts were obtained with a Horiba-Jobin Yvon LabRam HR instrument available at Lehigh University. The details of the instrument capability and wavenumber calibration procedure can be found elsewhere.[1] A 442 nm laser was used for spectra collection to minimize fluorescence from the SiO_2 supported catalysts. Approximately 15-20 mg of each catalyst powder was loaded into the sample cup of Harrick (HVC-DR2) environmental cell equipped with CF_2 optical window and O-ring sealing. The samples were first heated to 400 °C (heating rate 10 °C/min, hold time at 400 °C was 1 hour prior to any measurement) under flowing 10% O_2/Ar (Praxair, Certified Standard, 10% O_2/Ar balance; 30 mL/min flow rate). The Raman spectra of the catalysts were then collected by implementing 60 s/scan for a total of three scans to improve the signal to noise ratio.

c. Temporal analysis of products (TAP) experiment

The transient kinetic investigations of the catalysts were conducted in a TAP 3 instrument available at Idaho National Laboratory. Two different types of TAP experiments were conducted in this study. For these experiments, 50% $^{16}O_2$/He, $^{18}O_2$/Ar (50/50 mixture) and $^{13}CH_4$/Ar (50/50 mixture) gases were utilized. The 50% $^{16}O_2$/He gas cylinder was supplied by (Airgas, Idaho Falls, ID, USA, Certified Grade, 50±2% $^{16}O_2$/He balance). The $^{18}O_2$ and $^{13}CH_4$ isotope gases were procured from Sigma Aldrich (99% ^{18}O isotope and 99%

^{13}C isotope, respectively) and a 50/50 mixture with Ar (Airgas, Idaho Falls, ID, USA, Certified Grade, 99.999% Ar) was prepared using a lab-built gas blending system.

- *$^{16}O_2$-$^{18}O_2$ pump-probe experiment*

The $^{16}O_2$-$^{18}O_2$ pump-probe experiments were conducted within the Knudsen diffusion transport regime where no significant gas-phase interaction between the molecules is expected. Approximately, 15 mg of the catalyst was loaded into a quartz micro-reactor (I.D. ~4 mm, Length ~38 mm) and sandwiched between inert quartz particles of size 250-300 μm. Then the catalyst bed was evacuated to ~ 4 x 10^{-6} Pa, followed by heating to 800 °C (10 °C/min), with continuous pulsing of $^{16}O_2$/He and held at 800 °C for 30 minutes. Next, pulses of $^{16}O_2$/He (~ 2.7 x 10^{-9} moles/pulse) and $^{18}O_2$/Ar (~ 3 x 10^{-9} moles/pulse) were introduced into the catalyst bed in a pump-probe mode with pump-probe spacing of 2 s. The 2 s time delay between the pulses ensured complete removal of gas-phase $^{16}O_2$ before introduction of $^{18}O_2$ into the catalyst bed. Measurements of reactor gas exit flux was conducted using a mass-spectrometer (SRS RGA 200), situated at the exit of the micro-reactor. *m/z* values of 2 (*He*); 40 (*Ar*), 32 ($^{16}O_2$); 34 ($^{16}O^{18}O$) and 36 ($^{18}O_2$) were repeated in sequence. Additionally, the same experiments were repeated for different temperatures. In each case, results are shown after averaging over 12 to 15 pulses.

- *Anaerobic $^{13}CH_4$ series pulsing experiments*

The anaerobic $^{13}CH_4$ series pulsing experiment was conducted outside the conventional Knudsen diffusion limit to allow for gas phase coupling of $^{13}CH_3$• radicals for $^{13}C_2H_6$ generation. Isotopically labelled carbon was utilized to (*i*) minimize the interference of spurious outgassing from normal background N_2 level, and (*ii*) distinguish C_2 fragmentation from CO. For this experiment, ~ 25 mg of catalyst sample was used. The *in-situ* pre-treatment of the catalysts was carried out as previously described. After the pre-treatment step with $^{16}O_2$/He at 800 °C, the catalyst bed was maintained under high vacuum condition for 5 minutes to allow for removal of physisorbed O_2 species from the catalyst surface. Then, a series of $^{13}CH_4$/Ar pulses (~ 5.5 x 10^{-8} moles/pulse) was introduced into the reactor with simultaneous product measurement by online

mass-spectrometer. *m/z* values of 40 (*Ar*); 17 ($^{13}CH_4$); 29 (^{13}CO, $^{13}C_2H_6$ and $^{13}CO_2$); 30 ($^{13}C_2H_6$); 32 ($^{16}O_2$ and $^{13}C_2H_6$) and 45 ($^{13}CO_2$) were utilized. Separate calibration of mass-fragmentation values was used to deconvolute the overlapping masses of $^{13}C_2H_6$ and $^{16}O_2$ (for *m/z* = 32), $^{13}C_2H_6$ and ^{13}CO (for *m/z* = 29), and $^{13}CO_2$ and ^{13}CO (for *m/z* = 29).

$^{13}CH_4$ and $^{18}O_2$ conversion and OCM product selectivity and yield were calculated by the following formulae.

$$\%\ Conversion = \frac{(M_i - M_o)}{M_i} \times 100 \quad (1)$$

where, M_i and M_o are the inlet and outlet moles, respectively, of $^{13}CH_4$ or $^{18}O_2$.

$$\%\ Selectivity_j = \frac{m_{C_j}}{\sum m_{C_j}} \times 100 \quad (2)$$

where, m_{C_j} is the number of moles of carbon atoms in product j.

$$\%\ Yield_j = \frac{\%\ CH_4 Conversion \times \%\ Selectivity_j}{100} \quad (3)$$

2. Results and Discussion

a. *In-situ* Raman Spectroscopy

The *in-situ* Raman spectra of the catalysts are shown in **Figure S 1**. The dehydrated $5Na_2WO_4/SiO_2$ and $1.2Mn\text{-}5Na_2WO_4/SiO_2$ catalysts at 400 °C exhibit Raman bands at 925 and 805 cm^{-1}, corresponding to the crystalline phase of Na_2WO_4.[1,2] Additionally, a 665 cm^{-1} band is observed for $1.2Mn\text{-}5Na_2WO_4/SiO_2$ catalyst from the vibration of Mn_2O_3 phase.[3,4] The above two catalysts also possess bands from crystalline β-cristobalite phase of the SiO_2 support. In addition to the crystalline phases, a band ~ 946 cm^{-1} is also observed for these two catalysts, which originates from the presence of surface Na-WO_x sites.[1] Interestingly, the $0.5Na\text{-}5WO_x/SiO_2$ catalyst does not possess any crystalline Na_2WO_4 phase and exhibits only one Raman vibration ~ 958 cm^{-1}, from surface Na-WO_x sites.[1] On the other hand, the $1.2Mn/SiO_2$ catalyst has only one major vibration ~ 655 cm^{-1}, indicating the presence of Mn_2O_3 crystal phase.[3,4] The slight difference in vibration of Mn_2O_3 phase in $1.2Mn/SiO_2$ and $1.2Mn\text{-}5Na_2WO_4/SiO_2$ catalysts could be due to slight difference in their structure. In the literature, the Mn_2O_3 major Raman vibration has been reported to be present between 635 - 675 cm^{-1}.[3-5] The readers should note that at high temperature of OCM reaction environment, the Na_2WO_4 crystal melts and Mn_2O_3 crystal reduces to form amorphous Mn-oxide phase.[6-9]

In brief, our findings on the catalyst structure and their connection with the literature reports can be summarized as follows: In OCM reaction environment,

(i) The $0.5Na\text{-}5WO_x/SiO_2$ catalyst possesses only surface Na-WO_x sites over amorphous SiO_2 support.

(ii) The $1.2Mn/SiO_2$ catalyst possesses Mn-oxide phase on amorphous SiO_2 support.

(iii) The $5Na_2WO_4/SiO_2$ catalyst possesses two different types of active oxide phases, molten Na_2WO_4 and surface Na-WO_x sites, along with β-cristobalite phase of the SiO_2 support. Addition of Mn to this catalyst (for the supported $1.2Mn\text{-}5Na_2WO_4/SiO_2$ catalyst), contains additional Mn-oxide phase.

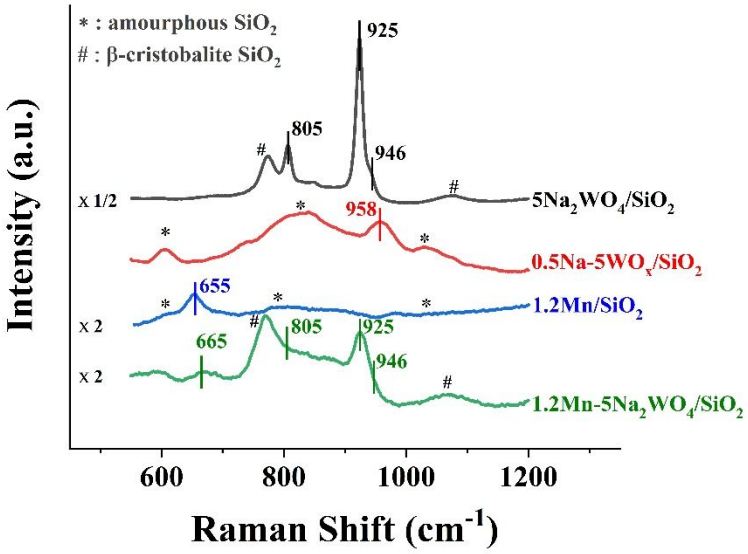

Figure S 1. Dehydrated Raman spectra (442 nm Laser) of the catalysts at 400 °C.

b. $^{16}O_2$-$^{18}O_2$ pump-probe experiment

Table S 1. $^{18}O_2$ conversion values for different catalysts and silica support materials at 800 °C during $^{16}O_2$-$^{18}O_2$ pump-probe experiment. Pump-probe spacing time is 2 s.

Catalyst	**$^{18}O_2$ Conversion (%)**
$5Na_2WO_4/SiO_2$	43
$0.5Na\text{-}5WO_x/SiO_2$	7.7
$1.2Mn/SiO_2$	32
$1.2Mn\text{-}5Na_2WO_4/SiO_2$	70
Bare SiO_2 support	~0
$0.8Na/SiO_2$ (Cristobalite SiO_2 phase)	~0

The isotopic yield of $^{16}O_2$, normalized by $^{18}O_2$ conversion, is shown in **Figure S 2** for the $5Na_2WO_4/SiO_2$ and $0.5Na\text{-}5WO_x/SiO_2$ catalysts. Corresponding $^{18}O_2$ conversion values at different temperatures are also included. For $0.5Na\text{-}5WO_x/SiO_2$ catalyst (explored in the temperature range of 700 to 800 °C), the ratio of $^{16}O_2$ desorbed to the $^{18}O_2$ converted is always ~ 1 at all temperatures, suggesting a closed oxygen balance for this catalyst. Interestingly, for the $5Na_2WO_4/SiO_2$ catalyst, the $^{16}O_2$ desorption amount is much higher than the $^{18}O_2$ converted. This is possible only if the bulk of the catalyst is also participating in the oxygen exchange process. Additionally, the high $^{16}O_2$ desorption to $^{18}O_2$ conversion ratio (~ 1.45 ± 0.05) is seen only above 700 °C, when Na_2WO_4 is present in molten state. At lower temperature values, 675 and 650 °C, this ratio progressively decreases towards 1. The slightly higher ratio at 675 °C could be due to the transition of molten to crystalline Na_2WO_4 phase.

The excessive desorption of $^{16}O_2$ from the $5Na_2WO_4/SiO_2$ catalyst, when molten Na_2WO_4 phase is present, warrants additional discussion. Many studies in the literature report the presence of dissolved gas phase species in the molten salt systems. For example, dissolved oxygen species has been reported to be present in molten salts of sodium (or alkali) carbonates, carbonate chlorides, sulfates, nitrates etc.[10-12] Additionally, carbon dioxide and sulfur dioxide are also found to be soluble in these molten salts. Also, the degree of dissolution of the gas phase molecules in these molten salts strongly depends on the temperature, gas phase partial pressure and other imposed experimental conditions, such as static gas environment *vs*. bubbling through or stirring of molten salts. These reports, in connection with our experimental findings, suggest that, (*i*) only the molten Na_2WO_4 phase is capable of holding and releasing dissolved molecular O_2 species, and (*ii*) when crystalline Na_2WO_4 or surface $Na\text{-}WO_x$ sites are present, the amount of dissolved O_2 species in the catalyst becomes negligible.

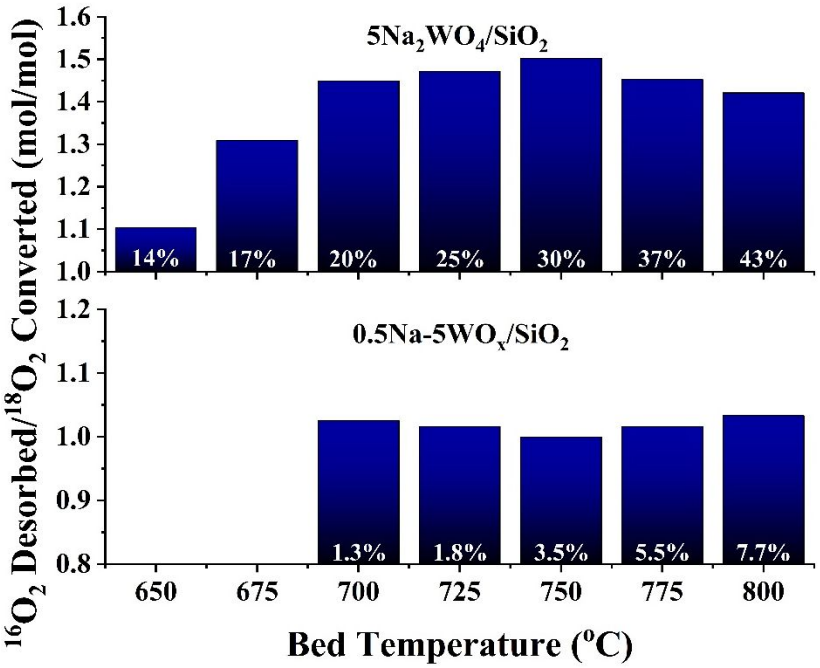

Figure S 2. Isotopic yield of $^{16}O_2$, normalized by $^{18}O_2$ conversion, for $5Na_2WO_4/SiO_2$ and $0.5Na\text{-}5WO_x/SiO_2$ catalysts. Corresponding $^{18}O_2$ conversion values at different temperatures are also included in the figure.

c. Anaerobic $^{13}CH_4$ series pulsing experiment

The mass-spectrometer signal response for $^{13}CH_4$ with pulse number, during an anaerobic $^{13}CH_4$ series pulsing experiment over $5Na_2WO_4/SiO_2$ catalyst, is shown in **Figure S 3**. The corresponding $^{13}CH_4$ conversion value is also included in the figure. The initial $^{13}CH_4$ conversion, ~2.9%, decreases with increasing pulse number and becomes negligible after 350 pulses. However, the dissolved $^{16}O_2$ desorption stopped after only pulse number 150 (see **Figure 2** in the main text). This suggests that a second type of catalytically active oxygen species (must be atomic O in nature) is present in the lattice of $5Na_2WO_4/SiO_2$ catalyst.

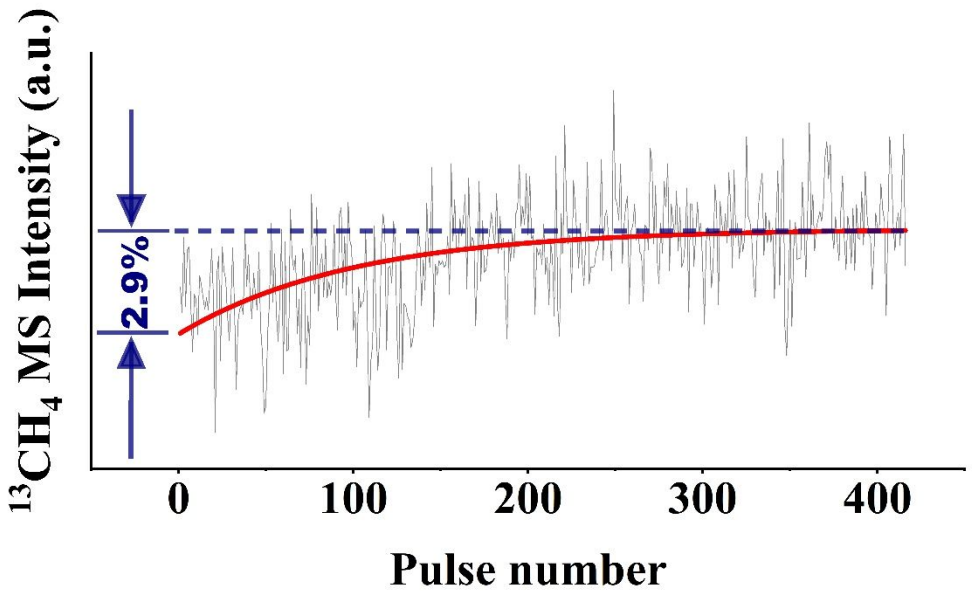

Figure S 3. Integrated mass-spectrometer response of $^{13}CH_4$ in anaerobic $^{13}CH_4$ series pulsing experiment over $5Na_2WO_4/SiO_2$ catalyst at 800 °C. The number shown in the plot represents the $^{13}CH_4$ conversion value at the start of the experiment.

The mass-spectrometer signal responses of various products with pulse number, during anaerobic $^{13}CH_4$ series pulsing experiment over 0.5Na-WO_x/SiO_2 catalyst, is shown in **Figure S 4**. **Figure S 4** (a) shows the $^{13}CH_4$ conversion over 0.5Na-WO_x/SiO_2 catalyst, with respect to the pulse number. From the figure it is clear that the initial $^{13}CH_4$ conversion of ~ 1% progressively decreases and goes to zero around pulse number ~ 150. The **Figure S 4** (b) shows the yield of various products in the same experiment. It can be seen that the 0.5Na-WO_x/SiO_2 catalyst does not release any dissolved molecular O_2 species, further supporting the fact that the dissolved O_2 species is associated with the molten Na_2WO_4 phase. ^{13}CO seems to be the major reaction product and its signal intensity goes down with number of $^{13}CH_4$ pulses and becomes insignificant after ~ 150 pulses. $^{13}C_2H_6$ and $^{13}CO_2$ MS signals are weak, yet formation of these molecules can be seen during the initial pulsing, which become zero ~ 90-100 pulse number.

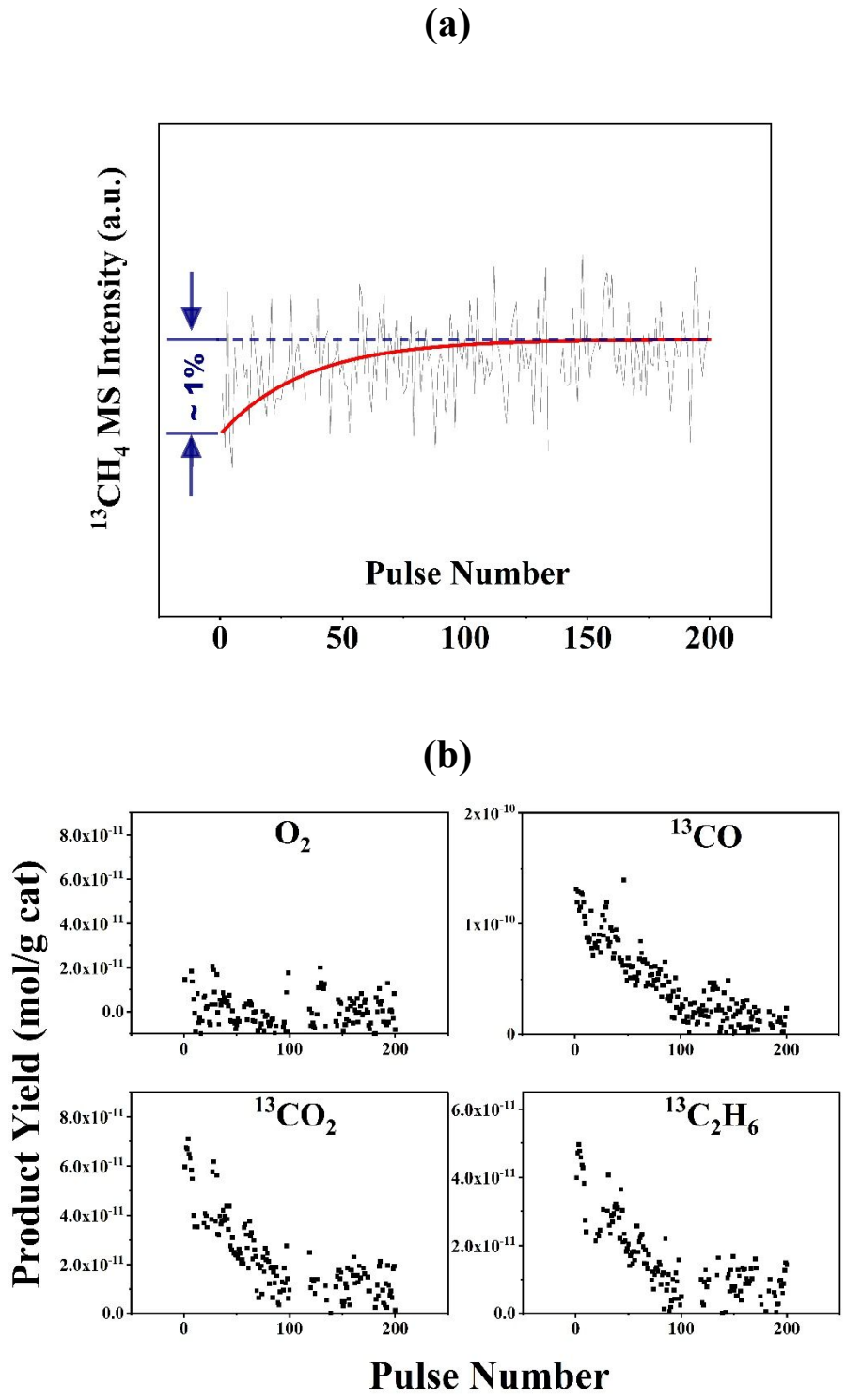

Figure S 4. (a) Integrated mass-spectrometer (MS) response of $^{13}CH_4$ and **(b)** Yield of various products during anaerobic $^{13}CH_4$ series pulsing experiment over 0.5Na-5WO_x/SiO_2 catalyst at 800 °C.

d. Effect of Support oxide phases

To understand any possible role of the support oxide phases in the oxygen exchange and activation, two additional samples were investigated, the amorphous bare SiO_2 support and the crystalline cristobalite phase of the SiO_2 support ($0.8Na/SiO_2$ catalyst). The $^{16}O_2$-$^{18}O_2$ pump-probe experiments conducted over these samples are shown in **Figure S 5**. From the figure it is clear that these oxide support phases are not capable of generating any dissolved molecular O_2 species. Additionally, no $^{18}O_2$ conversion is observed (see **Table S 1**) over these oxide support materials suggesting they are inert towards oxygen exchange between the catalyst oxide phase and the gas phase O_2.

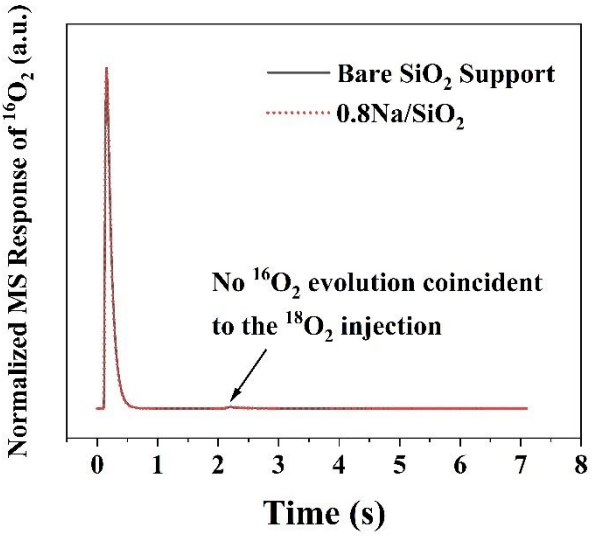

Figure S 5. Mass-spectrometer (MS) response of $^{16}O_2$ during $^{16}O_2$-$^{18}O_2$ pump-probe experiment (pump-probe spacing, $\Delta t = 2$ s).

Further, to investigate the CH_4 activation capability of the oxide support materials, $^{13}CH_4$ series pulsing experiments were conducted (see **Figure S 6** and **Figure S 7**). From **Figure S 6** (a) and **Figure S 7** (a) it is clear that the amorphous bare SiO_2 support and the $0.8Na/SiO_2$ (crystalline cristobalite SiO_2 phase) materials are not capable of activating CH_4 in the absence of gas phase O_2. Correspondingly, the OCM product evolutions over these samples, during $^{13}CH_4$ series pulsing experiment do not exhibit any responses beyond the background noise level (see **Figure S 6** (b) and **Figure S 7** (b)).

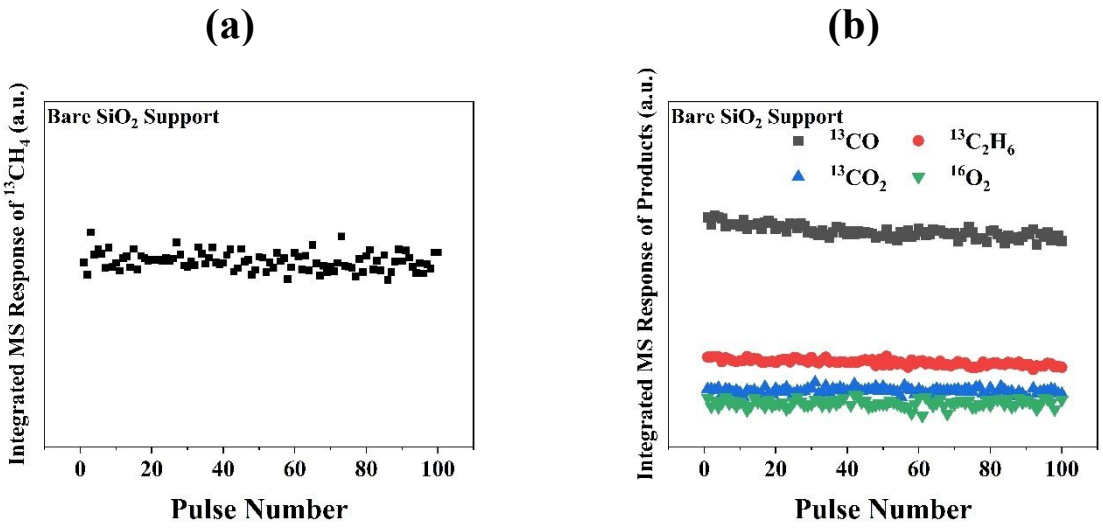

Figure S 6. (a) Integrated mass-spectrometer (MS) response of $^{13}CH_4$ and **(b)** various products during anaerobic $^{13}CH_4$ series pulsing experiment over the amorphous bare SiO_2 support at 800 °C. No change in the integrated mass-spectrometer signal for $^{13}CH_4$ and OCM products were observed with increasing pulse number.

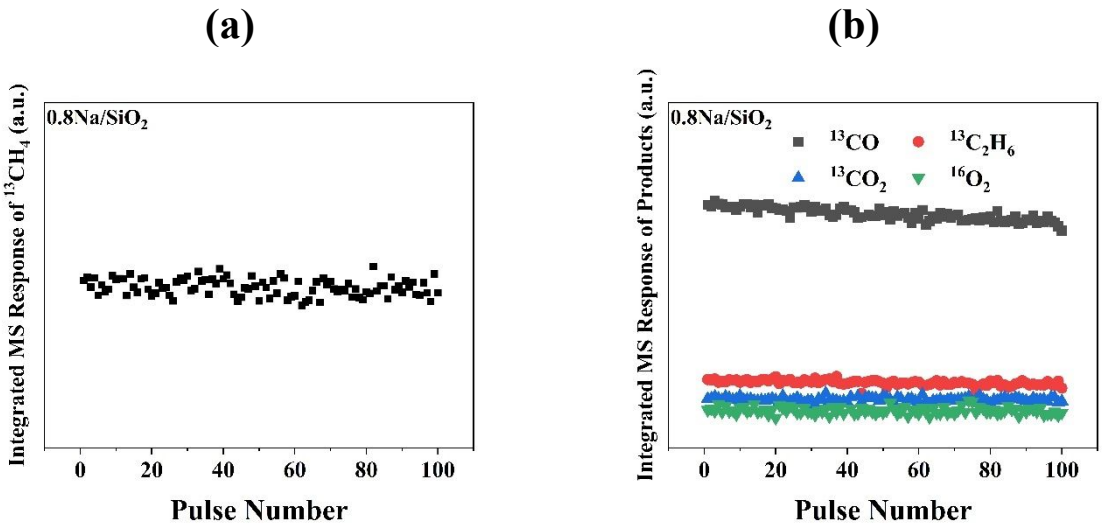

Figure S 7. (a) Integrated mass-spectrometer (MS) response of $^{13}CH_4$ and **(b)** various products during anaerobic $^{13}CH_4$ series pulsing experiment over $0.8Na/SiO_2$ sample with crystalline cristobalite SiO_2 phase at 800 °C. No change in the integrated mass-spectrometer signal for $^{13}CH_4$ and OCM products were observed with increasing pulse number.

e. Promotional Effect of Mn

To understand the individual role of Mn-oxide phase and the interaction between Mn-oxide and molten Na_2WO_4 phases in 1.2Mn-5Na_2WO_4/SiO_2 catalyst, $^{13}CH_4$ series pulsing experiments were conducted over 1.2Mn/SiO_2 and 1.2Mn-5Na_2WO_4/SiO_2 catalysts (see **Figure S 8** and **Figure S 9**, respectively). The corresponding data for 5Na_2WO_4/SiO_2 catalyst is shown in **Figure 2** and **Figure S 3**. Like the 5Na_2WO_4/SiO_2 catalyst, both 1.2Mn/SiO_2 and 1.2Mn-5Na_2WO_4/SiO_2 catalysts are capable of releasing molecular O_2 species in the absence of gas-phase oxygen. Interestingly, the release rate of O_2 species from the 1.2Mn/SiO_2 catalyst is much faster (see **Figure 3**) and all molecular O_2 species are released only in 20-25 pulses of $^{13}CH_4$. For 1.2Mn-5Na_2WO_4/SiO_2 catalyst, although the dissolved O_2 species release is observed up to pulse number 150, the total amount of O_2 released from this catalyst is much higher than the combined amount released from 5Na_2WO_4/SiO_2 and 1.2Mn/SiO_2 catalysts. This further confirms that in the presence of Mn, the Na_2WO_4 molten phase is capable of exchanging higher amount of dissolved molecular O_2 species (also observed for $^{16}O_2$-$^{18}O_2$ pump-probe experiments, see **Figure 3** in the main text) possibly via involvement of deeper dissolved oxygen species.

To further understand the catalytic roles of these dissolved O_2 species, the OCM product selectivity values were calculated, see **Figure 4** and **Figure S 10**. One can clearly see that the molecular O_2 species released from the Mn-oxide phase (1.2Mn/SiO_2 catalyst) is highly unselective towards C_2H_6 product formation and promotes the formation of CO. The dissolved O_2 and lattice atomic O species associated with the molten Na_2WO_4 phase and surface Na-WO_x sites (for 5Na_2WO_4/SiO_2 catalyst) possess much higher C_2H_6 selectivity (~ 25-30%). Interestingly, when Mn is present along with the molten Na_2WO_4 phase and surface Na-WO_x sites (for 1.2Mn-5Na_2WO_4/SiO_2 catalyst), the C_2 product selectivity improves significantly (becomes ~ 45-50%) indicating the Mn promotion on molten Na_2WO_4 phase and surface Na-WO_x sites.

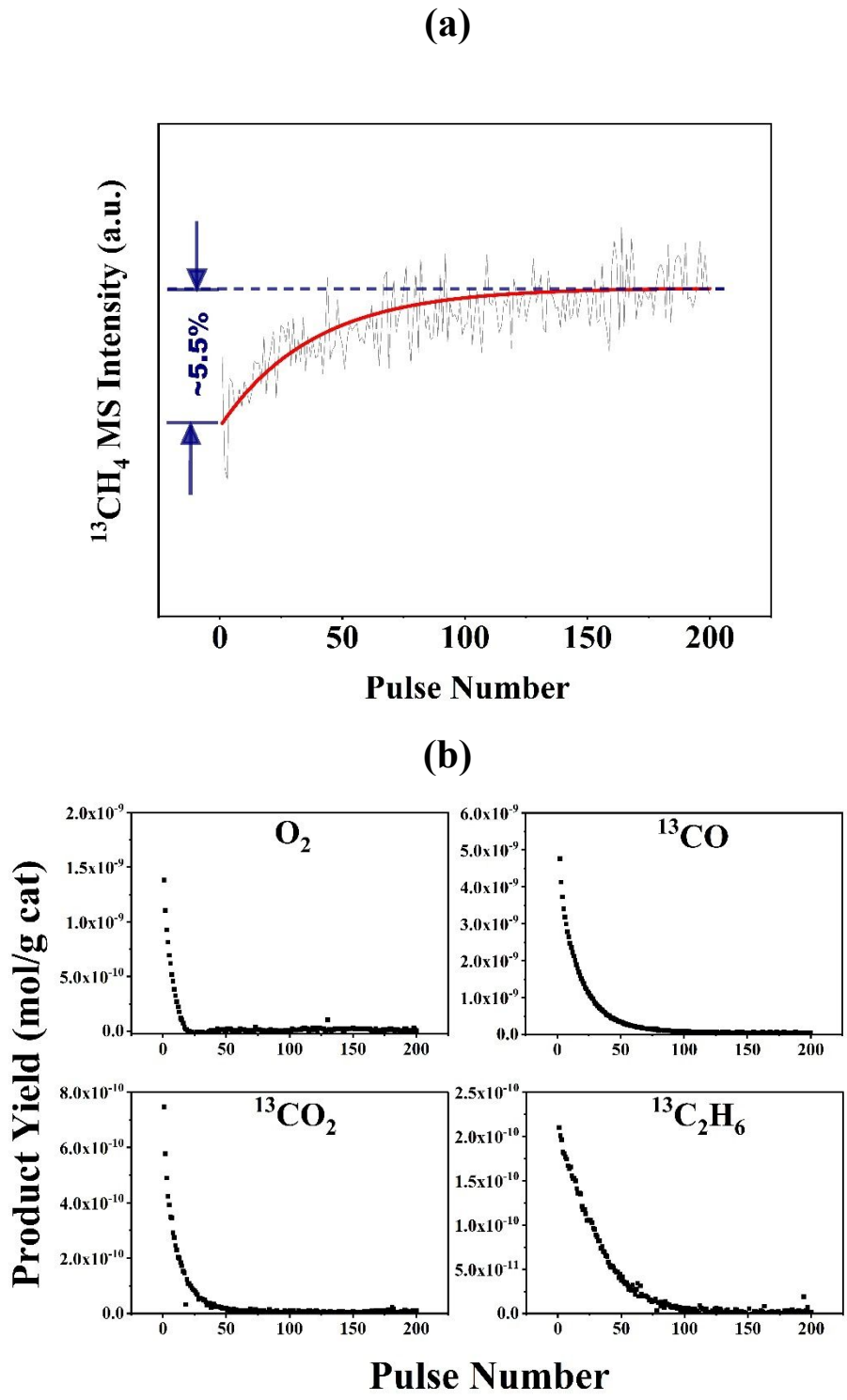

Figure S 8 (a) Integrated mass-spectrometer (MS) response of $^{13}CH_4$ and **(b)** Yield of various products during anaerobic $^{13}CH_4$ series pulsing experiment over 1.2Mn/SiO_2 catalyst at 800 °C.

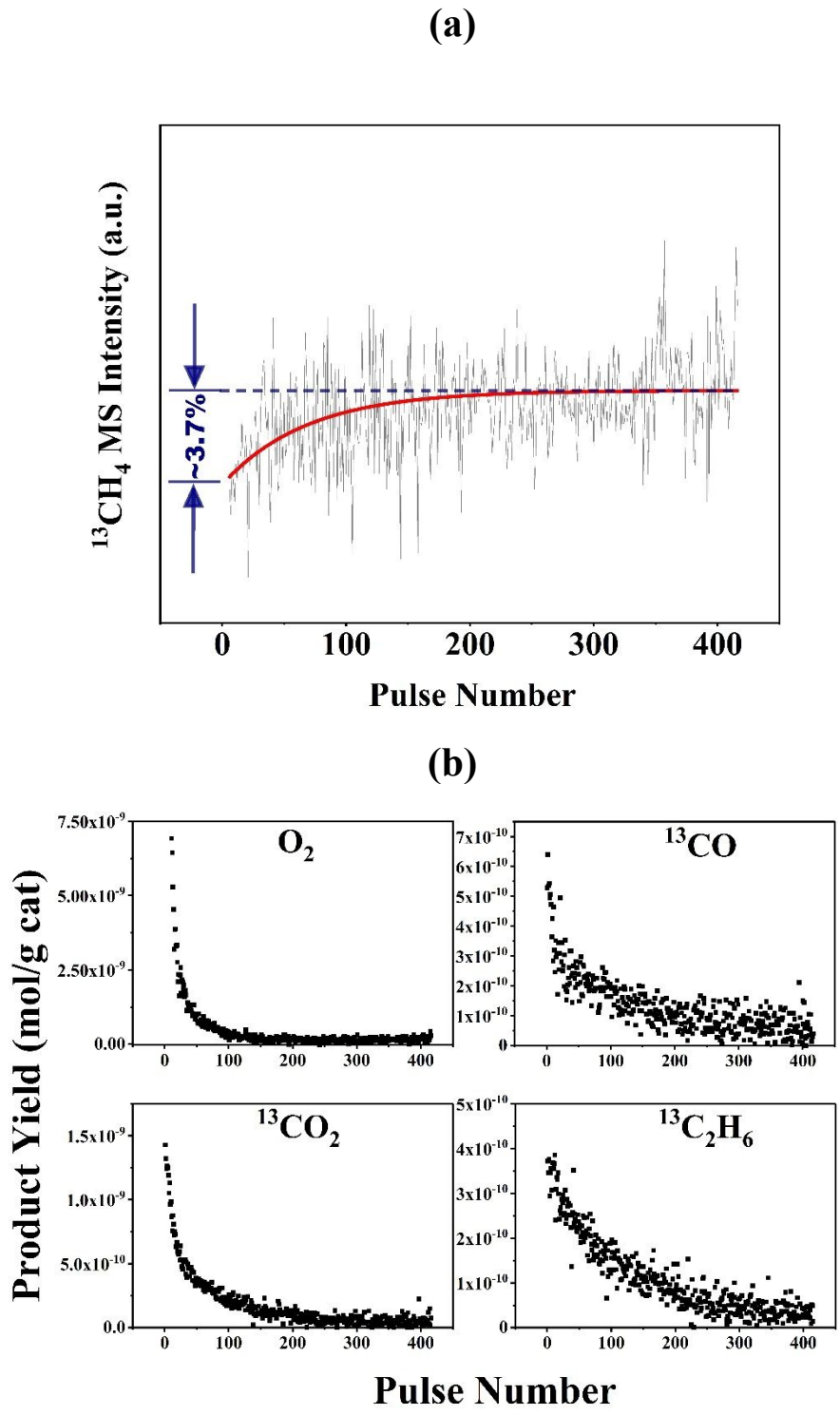

Figure S 9 (a) Integrated mass-spectrometer (MS) response of $^{13}CH_4$ and **(b)** Yield of various products during anaerobic $^{13}CH_4$ series pulsing experiment over 1.2Mn-5Na_2WO_4/SiO_2 catalyst at 800 °C.

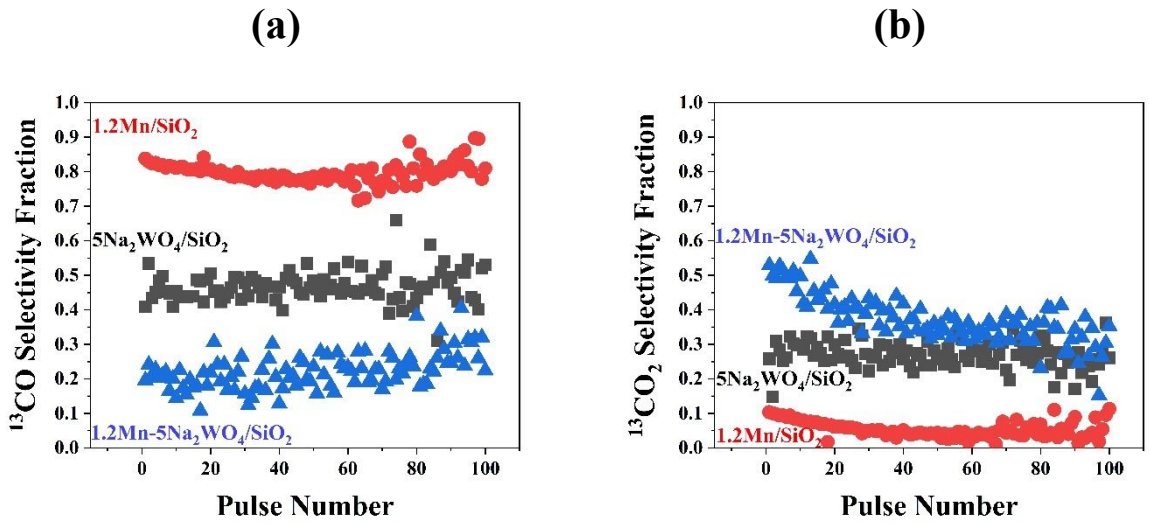

Figure S 10. (a) ^{13}CO and (b) $^{13}CO_2$ selectivity fraction for various catalysts. The original data used for this are presented in **Figure 2** ($5Na_2WO_4/SiO_2$ catalyst), **Figure S 8** ($1.2Mn/SiO_2$ catalyst) and **Figure S 9** ($1.2Mn\text{-}5Na_2WO_4/SiO_2$ catalyst).

The $^{16}O_2$ and $^{16}O^{18}O$ pulse response amounts from $5Na_2WO_4/SiO_2$, $1.2Mn/SiO_2$ and $1.2Mn\text{-}5Na_2WO_4/SiO_2$ catalysts during probe pulse of the $^{16}O_2$-$^{18}O_2$ pump-probe experiment are compared in **Figure S 11**. From **Figure S 11**, one can observe that (*i*) the $1.2Mn/SiO_2$ catalyst is also capable of desorbing molecular O_2 species, (*ii*) presence of Mn significantly increases the total amount of $^{16}O_2$ and $^{16}O^{18}O$ generation from $5Na_2WO_4/SiO_2$ catalyst. The higher $^{16}O_2$ response was attributed to the release of deeper dissolved O_2 species of Na_2WO_4 melt, in the presence of Mn (see **Figure 3** and associated discussion in the main text). However, the higher $^{16}O^{18}O$ generation warrants additional investigation. Since the absolute conversion values of $^{18}O_2$ were very different among these catalysts (see **Table S 1**), to understand the effect of Mn towards oxygen dissociation by forming $^{16}O^{18}O$ products, we investigated the $^{18}O_2$ conversion normalized $^{16}O^{18}O$ generation from these catalysts (see **Figure S 12**). The amount of $^{16}O^{18}O$ scrambled product formed over the $1.2Mn/SiO_2$ catalyst is much higher (5-6 x) than $5Na_2WO_4/SiO_2$ and $1.2Mn\text{-}5Na_2WO_4/SiO_2$ catalysts, suggesting the greater oxygen dissociation capability of Mn. However, when same weight loading Mn was added to the $5Na_2WO_4/SiO_2$ catalyst, the $^{16}O^{18}O$ generation per $^{18}O_2$ converted did not increase, indicating no effect of Mn towards oxygen dissociation present in $1.2Mn\text{-}5Na_2WO_4/SiO_2$ catalyst.

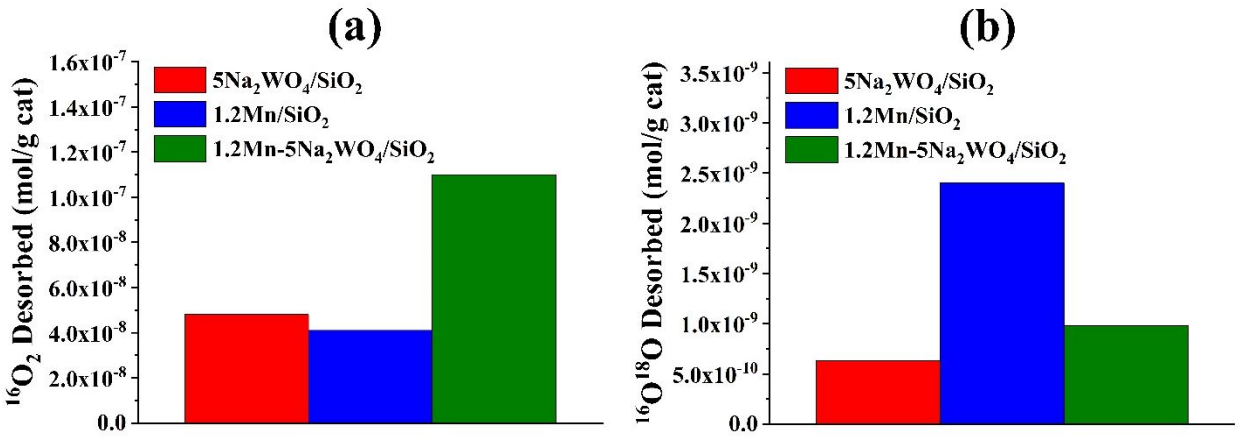

Figure S 11. (a) $^{16}O_2$ and **(b)** $^{16}O^{18}O$ generation over different catalysts during $^{16}O_2$-$^{18}O_2$ pump-probe experiment at 800 °C. The $^{16}O_2$ and $^{16}O^{18}O$ oxygen products were measured on the probe part of the experiment, coincident with the injection of secondary $^{18}O_2$ pulse.

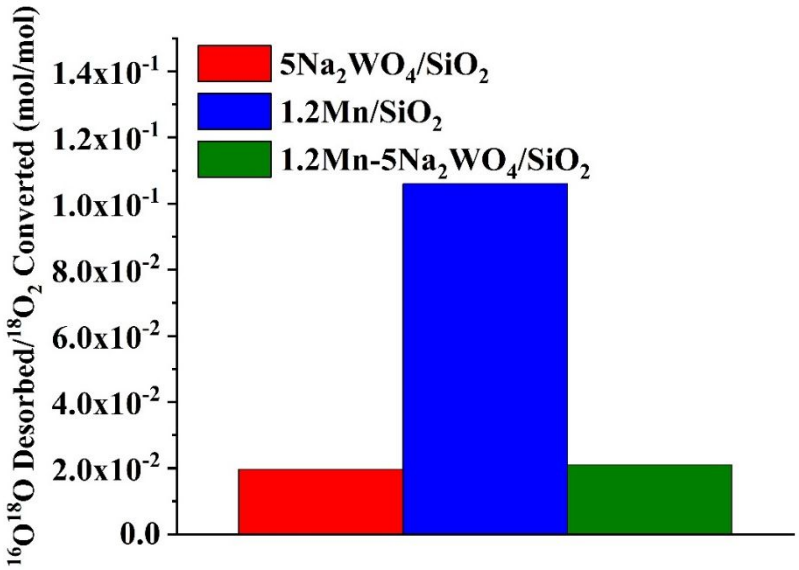

Figure S 12. $^{16}O^{18}O$ oxygen product generated per unit conversion of $^{18}O_2$ over various catalysts during $^{16}O_2$-$^{18}O_2$ pump-probe experiment at 800 °C. The $^{16}O^{18}O$ oxygen product generation was measured on the probe part of the experiment, coincident with the injection of secondary $^{18}O_2$ pulse.

References

1 Kiani, D., Sourav, S., Wachs, I. E. & Baltrusaitis, J. Synthesis and molecular structure of model silica-supported tungsten oxide catalysts for oxidative coupling of methane (OCM). *Catalysis Science & Technology* **10**, 3334-3345 (2020).

2 Ross-Medgaarden, E. I. & Wachs, I. E. Structural Determination of Bulk and Surface Tungsten Oxides with UV−vis Diffuse Reflectance Spectroscopy and Raman Spectroscopy. *The Journal of Physical Chemistry C* **111**, 15089-15099 (2007).

3 Julien, C. M., Massot, M. & Poinsignon, C. Lattice vibrations of manganese oxides: Part I. Periodic structures. *Spectrochimica Acta Part A: Molecular and Biomolecular Spectroscopy* **60**, 689-700 (2004).

4 Buciuman, F., Patcas, F., Craciun, R. & R. T. Zahn, D. Vibrational spectroscopy of bulk and supported manganese oxides. *Physical Chemistry Chemical Physics* **1**, 185-190 (1999).

5 Kapteijn, F., Vanlangeveld, A. D., Moulijn, J. A., Andreini, A., Vuurman, M. A., Turek, A. M., Jehng, J. M. & Wachs, I. E. Alumina-Supported Manganese Oxide Catalysts: I. Characterization: Effect of Precursor and Loading. *Journal of Catalysis* **150**, 94-104 (1994).

6 Hou, S., Cao, Y., Xiong, W., Liu, H. & Kou, Y. Site Requirements for the Oxidative Coupling of Methane on SiO_2-Supported Mn Catalysts. *Industrial & Engineering Chemistry Research* **45**, 7077-7083 (2006).

7 Vamvakeros, A., Jacques, S., Middelkoop, V., Di Michiel, M., Egan, C., Ismagilov, I., Vaughan, G., Gallucci, F., van Sint Annaland, M. & Shearing, P. Real time chemical imaging of a working catalytic membrane reactor during oxidative coupling of methane. *Chemical Communications* **51**, 12752-12755 (2015).

8 Matras, D., Vamvakeros, A., Jacques, S., Grosjean, N., Rollins, B., Poulston, S., Stenning, G. B. G., Godini, H., Drnec, J., Cernik, R. J. & Beale, A. M. Effect of thermal treatment on the stability of Na-Mn-W/SiO_2 Catalyst for the Oxidative Coupling of Methane. *Faraday Discussions* **229**, 176-196 (2021).

9 Vamvakeros, A., Matras, D., Jacques, S. D. M., di Michiel, M., Price, S. W. T., Senecal, P., Aran, M. A., Middelkoop, V., Stenning, G. B. G., Mosselmans, J. F. W., Ismagilov, I. Z. & Beale, A. M. Real-time multi-length scale chemical tomography of fixed bed reactors during the oxidative coupling of methane reaction. *Journal of Catalysis* **386**, 39-52 (2020).

10 Volkovich, V. A., Griffiths, T. R., Fray, D. J. & Thied, R. C. A new method for determining oxygen solubility in molten carbonates and carbonate–chloride mixtures using the oxidation of UO_2 to uranate reaction. *Journal of Nuclear Materials* **282**, 152-158 (2000).

11 Andresen, R. E. Solubility of Oxygen and Sulfur Dioxide in Molten Sodium Sulfate and Oxygen and Carbon Dioxide in Molten Sodium Carbonate. *Journal of The Electrochemical Society* **126**, 328-334 (1979).

12 Desimoni, E., Paniccia, F. & Zambonin, P. G. Solubility and detection (down to 30 p.p.b.) of oxygen in molten alkali nitrates. *Journal of Electroanalytical Chemistry and Interfacial Electrochemistry* **38**, 373-379 (1972).